Journal of Magnetic Resonance 198 (2009) 111–120

Contents lists available at ScienceDirect

Journal of Magnetic Resonance

journal homepage: www.elsevier.com/locate/jmr

Electron spin relaxation rates for semiquinones between 25 and 295 K in glass-forming solvents

Velavan Kathirvelu, Hideo Sato, Sandra S. Eaton *, Gareth R. Eaton

Department of Chemistry and Biochemistry, University of Denver, 2101 East Wesley Avenue, Denver, CO 80208, USA

ARTICLE INFO

Article history:
Received 16 March 2008
Revised 13 January 2009
Available online 30 January 2009

Keywords:
Electron spin relaxation
Molecular tumbling
Saturation recovery EPR
Semiquinone

ABSTRACT

Electron spin lattice relaxation rates for five semiquinones (2,5-di-t-butyl-1,4-benzosemiquinone, 2,5-di-t-amyl-1,4-benzosemiquinone, 2,5-di-phenyl-1,4-benzosemiquinone, 2,6-di-t-butyl-1,4-benzosemiquinone, tetrahydroxy-1,4-benzosemiquione) were studied by long-pulse saturation recovery EPR in 1:4 glycerol:ethanol, 1:1 glycerol:ethanol, and triethanolamine between 25 and 295 K. Although the dominant process changes with temperature, relaxation rates vary smoothly with temperature, even near the glass transition temperatures, and could be modeled as the sum of contributions that have the temperature dependence that is predicted for the direct, Raman, local mode and tumbling-dependent processes. At 85 K, which is in a temperature range where the Raman process dominates, relaxation rates along the g_{xx} ($g \sim 2.006$) and g_{yy} ($g \sim 2.005$) axes are about 2.7–1.5 times faster than along the g_{zz} axis ($g = 2.0023$). In highly viscous triethanolamine, contributions from tumbling-dependent processes are negligible. At temperatures above 100 K relaxation rates in triethanolamine are unchanged between X-band (9.5 GHz) and Q-band (34 GHz), so the process that dominates in this temperature interval was assigned as a local mode rather than a thermally activated process. Because the largest proton hyperfine couplings are only 2.2 G, spin rotation makes a larger contribution than tumbling-dependent modulation of hyperfine anisotropy. Since g anisotropy is small, tumbling-dependent modulation of g anisotropy makes a smaller contribution than spin rotation at X-band. Although there was negligible impact of methyl rotation on T_1, rotation of t-butyl or t-amyl methyl groups enhances spin echo dephasing between 85 and 150 K.

1. Introduction

Understanding of electron spin relaxation rates is needed for studies of interspin distances by relaxation enhancement [1] and for design of experiments such as electron–nuclear double resonance [2] and electron–electron double resonance [3]. Early fundamental work on electron spin lattice relaxation was based on ions in a crystalline lattice, as summarized in references [4–6]. Subsequent studies have found that the characteristic temperature dependence predicted for these solid state mechanisms also is observed in glassy solvents [7–9] for triarylmethyl [10,11], nitroxyl [12–14], and galvinoxyl [12] radicals, and for Cu(II) [15] and V(IV) complexes [16].

The contribution from the one-phonon direct process, which often dominates at low temperatures, increases linearly with temperature.

$$\frac{1}{T_1^{\mathrm{dir}}} = C_{\mathrm{dir}} T \tag{1}$$

Contributions to relaxation with this linear temperature dependence have been found to increase with spin concentration [13], which suggests that intermolecular spin–spin interaction can be significant. For a vanadyl porphyrin the contribution from the direct process increased with increasing Larmor frequency [17].

The two-phonon Raman process for $S = ½$ [18] has the characteristic temperature dependence [19,20]:

$$\frac{1}{T_1^{\mathrm{Ram}}} = C_{\mathrm{Ram}} \left(\frac{T}{\theta_{\mathrm{D}}}\right)^9 J_8\left(\frac{\theta_{\mathrm{D}}}{T}\right) \quad \text{where} \quad J_8\left(\frac{\theta_{\mathrm{D}}}{T}\right) = \int_0^{\theta_{\mathrm{D}}/T} x^8 \frac{e^x}{(e^x-1)^2}\,dx \tag{2}$$

where θ_{D} is the effective Debye temperature in K and J_8 is the transport integral. In the derivation of the direct and Raman processes the Debye temperature is the upper cutoff frequency for the phonon distribution. Especially in molecular solids, there is not a sharp cutoff frequency, so the Debye temperature determined by fitting to experimental data is an 'effective' Debye temperature that is characteristic of a particular sample [21]. The effective Debye temperatures in glasses usually are lower than in ionic lattices and often are between 30 and 150 K [7]. The high temperature limiting behavior

* Corresponding author. Fax: +1 303 871 2254.
E-mail addresses: seaton@du.edu, sandra.eaton@du.edu (S.S. Eaton).

1090-7807/$ - see front matter © 2009 Elsevier Inc. All rights reserved.
doi:10.1016/j.jmr.2009.01.026

of the Raman process, which is observed above the Debye temperature, is

$$\frac{1}{T_1^{\mathrm{Ram}}} = C'_{\mathrm{Ram}} T^2 \tag{3}$$

Temperature regions in which $1/T_1$ increases proportional to T^2 are well defined for triarylmethyl [10,11] and nitroxyl [7,12] radicals in glassy solvents.

In glassy solvents at higher temperatures, but where the molecule is still tumbling slowly on the EPR time scale, $1/T_1$ increases with temperature more rapidly than the T^2 dependence of the Raman process, which could arise from a local mode as described by Eq. (4) [22] or a thermally activated process as described by Eq. (5) [9].

$$\frac{1}{T_1^{loc}} = C_{loc} \frac{\exp[\frac{\Delta_{\mathrm{loc}}}{T}]}{(\exp[\frac{\Delta_{\mathrm{loc}}}{T}] - 1)^2} \tag{4}$$

where Δ_{loc} is the energy of the local mode in K. If C_{loc} is independent of Larmor frequency, the contribution from the local mode is frequency independent.

$$\frac{1}{T_1^{\mathrm{therm}}} = C_{\mathrm{therm}} \frac{\tau_{\mathrm{therm}}}{1 + \omega^2 \tau_{\mathrm{therm}}^2} \tag{5}$$

where ω is the Larmor frequency, τ_{therm} is the correlation time for the dynamic process = $\tau_c^0 \exp(E_a/RT)$, E_a is the activation energy, and τ_c^0 is the pre-exponential factor. Unless the coefficient C_{therm} has a frequency dependence that compensates for the frequency dependence of the spectral density function in Eq. (5), the contribution from a thermally activated process is frequency dependent. For a limited temperature range at a single Larmor frequency, it is difficult to distinguish between the temperature dependence of relaxation due to a thermally activated process or a local mode. However, the two processes can be distinguished based on the frequency dependence of the thermally activated process and the frequency independence of the local mode [8].

For triarylmethyl radicals [11], nitroxyl radicals [12], bis-diethyldithiocarbamato(Cu(II)) [17], and a vanadyl porphyrin [17] a frequency-independent process is observed, which is therefore assigned to a local mode. For radicals with large hyperfine couplings to methyl protons, rotation of the methyl groups at a rate comparable to the Larmor frequency enhances $1/T_1$, which is a thermally activated process [23,24]. Enhancement of $1/T_1$ below about 20 K by methyl tunneling has been observed [25,26].

Above the glass transition temperature, as the rate of molecular tumbling becomes faster, two additional processes may become significant – spin rotation (Eq. (6)) [27] and modulation of g and A anisotropy by tumbling (Eq. (7)) [28–32].

$$\frac{1}{T_1^{\mathrm{SRot}}} = \frac{\sum_{i=1}^{3} (g_i - g_e)^2}{9\tau_{\mathrm{R}}} \tag{6}$$

where τ is the tumbling correlation time and $i = x, y, z$.

$$\frac{1}{T_1^{g,A}} = C_{A,g} \frac{\tau}{1 + (\tau\omega)^2} \tag{7}$$

where ω is the electron Larmor frequency.

$$C_{A,g} = \frac{2}{5\hbar^2} \left(\frac{\Delta g^2}{3} + \delta g^2 \right) \mu_B^2 B^2 + \frac{2}{9} I(I+1) \sum_i (\mathrm{A}_i - \bar{\mathrm{A}})^2 \tag{8}$$

where I is the nuclear spin, $\bar{A}$ is the average nuclear hyperfine coupling, and A_i is the x, y, or z component of the nuclear hyperfine coupling.

$$\Delta g = g_{zz} - 0.5(g_{xx} + g_{yy}) \quad \text{and} \quad \delta g = 0.5(g_{xx} - g_{yy}) \tag{9}$$

For nitroxyl radicals in the absence of O_2, the dominant tumbling-dependent contribution to relaxation is modulation of g and A anisotropy [14,30,33,34]. Tumbling correlation times for nitroxyl radicals can be determined by simulation of lineshapes in CW spectra [35]. For nitroxyl $\tau > 10^{-9}$ s modeling of spin lattice relaxation rates requires a tumbling-independent contribution that has been proposed to be thermally activated methyl rotation [30], solvent spin diffusion [28,36], or a combination of Raman process and local mode [14]. For triarylmethyl radicals g values are close to g_e and hyperfine interactions are small, so tumbling-dependent processes make negligible contribution to $1/T_1$ at X-band and the dominant contribution, even in water at room temperature, has the temperature dependence that is characteristic of a local mode [10,11]. For triarylmethyl radicals at 250 MHz $\omega\tau$ is ~1 at ambient temperature so modulation of weak hyperfine interactions makes larger contributions to $1/T_1$ than at X-band [37].

Semiquinones are important in a variety of biological systems [38,39]. Knowledge of semiquinone relaxation rates is needed for relaxation enhancement measurements of interspin distances such as between the iron-sulfur cluster and the flavin adenine dinucleotide (FAD) semiquinone of electron transfer flavoprotein ubiquinone oxidoreductase (ETF-QO) [40,41]. There are a few reports in the literature concerning the temperature dependence or mechanism of spin lattice relaxation of semiquinones [42–48] at temperatures between about 200 K and room temperature at X-band. The dependence of semiquinone relaxation on microwave frequency was tested only at room temperature [46]. Values of the spin lattice relaxation rate, $1/T_1$, obtained by pulse methods as a function of temperature and viscosity [42–44,46,47] have been fitted with Eq. (10).

$$\frac{1}{T_1} = A\frac{T}{\eta} + Be^{E_a/RT} \tag{10}$$

where η is viscosity and E_a is activation energy. There is general agreement that the term containing T/η is due to spin rotation. However the second term is not well understood and has been attributed to hindered rotation [43,47], and/or spin rotation [46].

To better understand relaxation processes for semiquinones, relaxation rates for five semiquinones (Table 1) were measured by long-pulse saturation recovery (SR) between 25 K and room temperature and by electron spin echo (ESE) between about 85 K and room temperature. The semiquinones were selected to vary the positions of substitution on the ring, the magnitude of proton hyperfine couplings, and the presence or absence of methyl groups that could undergo dynamic processes on the time scale of the experiments (Table 1). To vary the magnitude of the tumbling-dependent contribution to $1/T_1$ three solvents systems were selected that have increasing viscosities at room temperature: 1:4 glycerol:ethanol, 1:1 glycerol:ethanol, and triethanolamine. Because of differences in solubilities and stabilities it was not possible to study all of the semiquinones in all of the solvents. Data at X-band and Q-band were compared to distinguish between proposed mechanisms. Room temperature SR measurements also were performed at S-band. Since spin echo dephasing rates can provide complementary information about molecular dynamics, values of $1/T_m$ were measured for the series of semiquinones.

2. Experimental

2.1. Preparation of samples

2,5-Di-t-butyl-hydroquinone (98%, Alfa Aesar), 2,6-di-t-butyl-1,4-benzoquinone (98%, Aldrich), 2,3,5,6-tetrafluro-1,4-benzoquinone (97%, Aldrich Chemical Co.), 2,5-di-t-amyl-1,4-benzoquinone

Table 1
Semiquinones studied.

Name	Structure	Molar mass (g/mol)	Isotropic ^{1}H hyperfine (G) ±0.002	Anisotropic ring ^{1}H hyperfine (G) ±0.1
THSQ	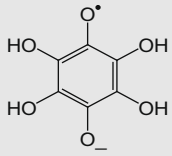	172		
2,6tBSQ	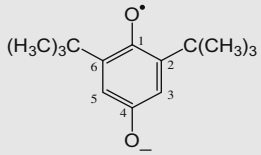	220	0.052 (18 H) 1.24 (2 H)	A_{xx} = 1.28 A_{yy} = 0.92 A_{zz} = 1.44
2,5tBSQ	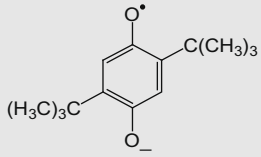	220	0.056 (18 H) 2.15 (2 H)	A_{xx} = 2.14 A_{yy} = 1.92 A_{zz} = 2.35
2,5tASQ	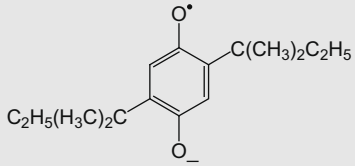	250	2.14 (2H)	A_{xx} = 2.13 A_{yy} = 2.03 A_{zz} = 2.35
2,5PSQ	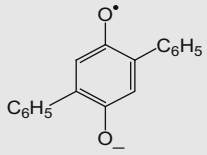	260	2.21 (2H)	A_{xx} = 2.68 A_{yy} = 2.07 A_{zz} = 2.88

(TCI America), 2,5-di-phenyl-1,4-benzoquinone (TCI America), 4-hydroxy-2,2,6,6-tetramethylpiperidin-1-yl (tempol) (Aldrich Chemical Co.) and 4-oxo-2,2,6,6-tetramethylpiperidin-1-yl (tempone) (Aldrich Chemical Co.) were used without further purification.

2,5-Di-t-butyl-1,4-benzosemiquinone (2,5tBSQ) was prepared by air oxidation at pH 12 by mixing equal volumes of air-saturated solutions of the corresponding hydroquinone and KOH [49], followed immediately by freeze-pump-thaw-degassing of the solution. The 2,6-di-t-butyl-1,4-benzosemiquinone (2,6tBSQ) and 2,5-di-t-amyl-1,4-benzosemiquinone (2,5tASQ) also were prepared by air oxidation of the corresponding quinones.

Tetrahydroxy benzosemiquinone (THSQ) was prepared by mixing one equivalent of air saturated triethanolamine solution of 2,3,5,6-tetrafluro-1,4-benzoquinone with five equivalents of KOH. 2,5-Di-phenyl-1,4-benzoquinone was reduced to hydroquinone with sodium dithionite, and semiquinone (2,5PSQ) was then generated by air oxidation as described above.

2.2. EPR spectra

Samples were degassed by freeze-pump-thaw. Relaxation rates at 0.2 and 0.5 mM are the same, within experimental error, which indicates negligible concentration dependence in this range. To improve signal-to-noise ratios, concentrations typically were about 0.5 mM.

2.2.1. CW spectra

X-band CW spectra were recorded on a Varian E9 spectrometer with a rectangular TE_{102} cavity. A modulation frequency of 25 kHz was used to avoid modulation broadening. DPPH (g = 2.0036) was used as the g value standard at X-band. Spectra were simulated using locally written software to determine hyperfine coupling constants and g values. To more accurately determine anisotropic g values Q-band CW spectra were obtained on a Bruker E580 spectrometer with a split ring resonator using 10 kHz modulation. The average of the g values obtained from the Q-band spectra was adjusted to match the calibrated g_{iso} values obtained at X-band.

2.2.2. Pulsed EPR

X-band spin lattice relaxation rates ($1/T_1$) were measured on a locally constructed SR spectrometer [50] using a rectangular cavity with $Q \sim 3000$. Q-band measurements were performed on a Bruker E580. Relaxation rates as a function of temperature were measured at the magnetic field position that corresponds to the maximum intensity in the absorption spectrum. Observe power was reduced until further decrease had no impact on apparent T_1. Below about 25 K the relaxation times of semiquinones are longer than about 50 ms. The attenuation available on the spectrometer was not sufficient to decrease the observe power to the low levels required to avoid perturbing the recovery curves for such long values of T_1. Therefore measurements were performed between 25 and 295 K. In order to avoid contributions from spectral diffusion to the recovery signal, the pump pulse was longer than T_1. Pump times ranged from 40 ms at 25 K to 20 μs at 298 K for 2,6tBSQ in 1:4 glycerol:ethanol, for example. Artifacts due to switching and cavity heating were removed by subtraction of an off-resonance signal. The time windows used to record recovery signals were 10 times T_1. Single exponentials gave good fits to the recovery curves.

The X-band spin lattice relaxation rates for 2,5tBSQ and THSQ in triethanolamine also were measured by inversion recovery with a

π-T_{var}-$\pi/2$-τ-π-τ-echo pulse sequence on a Bruker E580 spectrometer, using an over-coupled split ring resonator. Measurements were made using 20 ns, 10 ns, 20 ns pulses. The time windows used to record the inversion recovery signals were 10 times T_1. The values of T_1 obtained by inversion recovery in the center of the spectra between 85 and 300 K were 10–15% longer than the values measured by long-pulse SR. Inversion recovery signals are more susceptible to the effects of spectral diffusion than SR signals because the inverting pulse is short [8]. However, spectral diffusion would be expected to decrease, rather than increase, the apparent T_1 so differences between T_1 values obtained by SR and inversion recovery are not due to spectral diffusion. The 10 ns $\pi/2$ pulses produce a B_1 of about 9 G, which is much larger than the B_1 for the SR experiments. As discussed below, T_1 is longer along g_{zz} than along g_{xx} or g_{yy}. The X-band T_1 values were measured in the center of the spectrum, which is dominated by g_{xx} and g_{yy}. The systematically longer values of T_1 obtained by inversion recovery are attributed to the broader excitation bandwidth which averaged in longer contributions from other orientations. Data used to analyze the temperature dependence of $1/T_1$ and shown in the figures were obtained by SR unless noted otherwise.

S-band SR measurements at room temperature were performed on a locally designed spectrometer [51] using a loop gap resonator with $Q \sim 2900$.

Two-pulse echo decays were measured on a Bruker E580 spectrometer using a split ring resonator with $Q \sim 500$ that was over-coupled to $Q \sim 150$. Measurements were made using 40 and 80 ns pulses and detection windows about 10 times T_m. Initial times for data acquisition were 100 ns.

In 1:1 and 1:4 glycerol:ethanol relaxation rates for the semiquinones were the same for samples that were gradually cooled and ones that were rapidly cooled and then gradually warmed. Solutions in triethanolamine became cloudy if the solution was cooled slowly between about 260 and 280 K. Relaxation rates in triethanolamine above about 280 K were obtained by slow cooling from room temperature. Rates at lower temperatures were obtained by cooling quickly in liquid nitrogen and then gradually warming the sample.

2.3. Tumbling correlation times

The glass transition temperatures for the solvent mixtures that were used in this study have not been reported in the literature. The temperatures above which the line shapes of the CW spectra for tempol become more temperature dependent are about 180 K for 1:4 glycerol:ethanol and about 218 K for 1:1 glycerol:ethanol. These temperatures are below the point where tumbling was observed to make a significant contribution to $1/T_1$.

Since methods have not been developed to calculate the tumbling correlation times of semiquinones from CW EPR spectra, it was assumed that tumbling times for the semiquinones would be proportional to those of a nitroxyl. For nitroxyl radicals in 1:1 water:glycerol tumbling correlation times, τ, follow the Stokes–Einstein model with addition of a slip coefficient c_{slip}, $\tau = c_{slip}V\eta/kT$ where V is molecular volume, and η is viscosity [14]. The slip coefficient depends on both solvent and solute and ranges between 0.02 and 0.12 for tempone in various solvents. The X-band CW spectra of tempone and tempol were recorded as a function of temperature in the same solvents that were used for the semiquinone experiments, and the nitroxyl lineshapes were simulated using the NLSL program [35] to estimate the rotational diffusion rates $R_{||}$ and $R_{\perp}$. The parameters needed for the NLSL simulations (g_{zz}, g_{yy}, g_{xx}, A_{zz}, A_{yy}, A_{zz}) were obtained by simulating frozen solution spectra using locally written software. Rotational anisotropy was significant only at lower temperatures where the tumbling-dependent contributions to $1/T_1$ were small. Isotropic motion was therefore assumed in analyzing relaxation, and the tumbling correlation times were obtained from the rotational diffusion rates using the expression $\tau = 1/(6[R_{||}R_{\perp}^2])^{1/3}$.

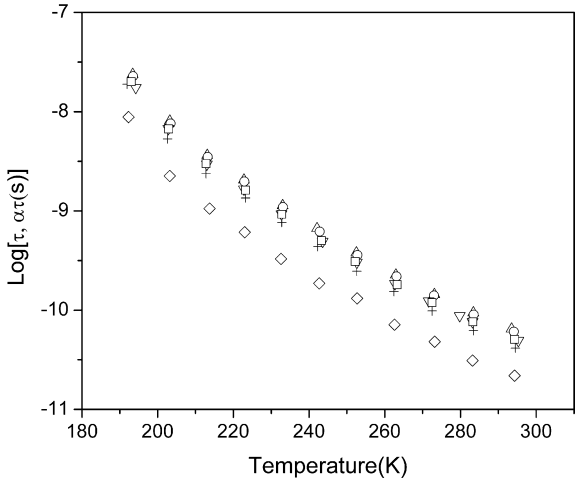

Fig. 1. Temperature dependence of tumbling correlation times τ in 1:4 glycerol:ethanol for tempone (◇) and tempol (+) obtained by simulation of CW lineshapes and $\alpha\tau$ for 2,5tBSQ (▽), 2,5tASQ (○), 2,5PSQ (△), and 2,6tBSQ (□) obtained by analysis of the temperature dependence of $1/T_1$.

The temperature dependence of τ for tempol and tempone in 1:4 glycerol:ethanol is shown in Fig. 1. Although the molar masses differ by only 2 amu, the τ values for tempol are about twice as large as for tempone, which demonstrates the effect of hydrogen bonding on c_{slip}. Since hydrogen bonding is significant for the semiquinones, it was assumed that values of τ for semiquinones were proportional to values for tempol. The curves for tempone and tempol in Fig. 1 are parallel, so the use of tempone instead of tempol to estimate τ for semiquinones would only increase values of α in Eqs. (12) and (13) and would not otherwise change the fit functions.

2.4. Analysis of the temperature dependence of $1/T_1$

The temperature dependence of the relaxation rates was modeled as the sum of contributions (Eq. (11)) from the direct process (Eq. (1)), Raman process (Eq. (2)), local mode (Eq. (4)), spin rotation (Eq. (12)), and modulation of g and A anisotropy (Eq. (13)).

$$\frac{1}{T_1} = \frac{1}{T_1^{dir}} + \frac{1}{T_1^{Ram}} + \frac{1}{T_1^{loc}} + \frac{1}{T_1^{SRot}} + \frac{1}{T_1^{g,A}} \tag{11}$$

$$\frac{1}{T_1^{SRot}} = \frac{\sum_{i=1}^{3}(g_i - g_e)^2}{9\alpha\tau} \tag{12}$$

$$\frac{1}{T_1^{g,A}} = C_{A,g}\frac{\alpha\tau}{1 + (\alpha\tau\omega)^2} \tag{13}$$

Eqs. (12) and (13) for the tumbling-dependent processes were modified from Eqs. (6) and (7) by using $\alpha\tau$ instead of τ, where τ is the tumbling correlation time for tempol in the same solvent at that temperature, and α is the scaling factor that relates the semiquinone tumbling time to that for tempol. For nitroxyl radicals in fluid solution [14] it was observed that the Cole–Davidson (CD) spectral density function [52], which was developed for dielectric relaxation, was a better model than the Bloembergen Pound Purcell (BPP) spectral density function. For the semiquinones the contribution from modulation of g and A anisotropy (Eqs. (7) and (13)) is so small that it was not possible to distinguish between the models, so the simpler BPP spectral density function was used.

Each of these processes predicts a distinctive dependence of $1/T_1$ on temperature and tumbling correlation time. C_{dir} (Eq.

(1)), C_{Ram} (Eq. (2)), and C_{loc} (Eq. (4)) are adjustable parameters that scale the contributions from the corresponding processes. The other adjustable parameters are θ_D, Δ_{loc}, and α. These six parameters were varied to give the best least-squares fit to the plots of $\log(1/T_1)$ vs. $\log T$. The dominant contribution changes with temperature. In the initial analyses all parameters were varied, and values were selected based on the goodness of fit in the temperature regime where a particular process dominated. Based on these analyses θ_D, ranged from 148 to 155 K and Δ_{loc} ranged from 595 to 607 K; these variations are less than the uncertainties in the values. Values of C_{Ram} and θ_D are correlated, so to permit comparisons of C_{Ram}, independent of θ_D, θ_D was fixed at 150 K. Values of C_{loc} and Δ_{loc} are correlated, so to permit comparisons of C_{loc}, independent of the energy of the local mode, Δ_{loc} was fixed at 600 K. The use of the average values of θ_D and Δ_{loc} instead of the extreme values corresponds to an uncertainty of about 5% in the coefficients C_{Ram} or C_{loc}. Although extrapolation of the T^2 dependence of the Raman process above the glass transition temperature is not proven, substantial deviation from T^2 results in coefficients of other processes that seem less physically reasonable. It is expected that as more relaxation information is obtained for organic radicals in fluid solution, additional mechanisms will be identified that may suggest refinement of the coefficients reported here. The tumbling scaling parameter α in Eq. (12) was determined by first adjusting C_{Ram} and C_{loc} to match the relaxation rates at temperatures where the contribution from the tumbling-dependent process is negligible, and then adjusting α to minimize the error function at higher temperatures. The resulting parameters are given in Table 2. Values of α (Table 2) are in the range of 1.23–1.5 and correlate with trends in molecular weight, as expected. The values of $\alpha\tau$ for four semiquinones in 1:4 glycerol:ethanol (Fig. 1) gave good fit to the tumbling-dependent contributions to relaxation as discussed below.

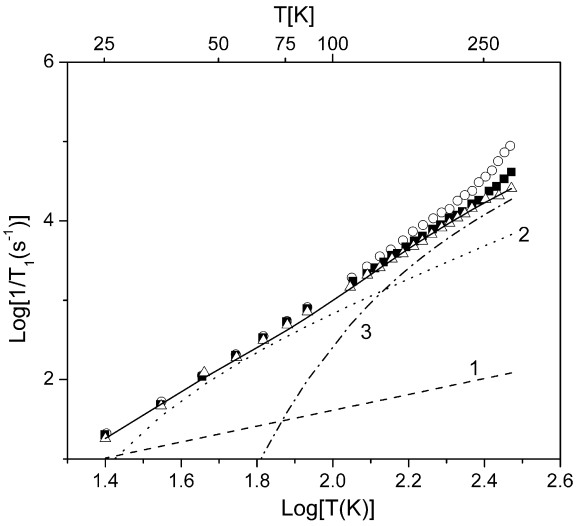

Fig. 2. Temperature dependence of relaxation rates at X-band for 2,5tASQ in 1:4 glycerol:ethanol (○), 1:1 glycerol:ethanol (■), and triethanolamine (△). The solid line is the fit function and the dashed lines are the contributions from the direct (1), Raman (2), and local-mode processes (3), respectively, in triethanolamine. It is assumed that the temperature dependence that is characteristic of the Raman and local modes in glasses persists above the glass transition temperature.

3. Results and discussion

3.1. Temperature dependence of $1/T_1$

X-band spin–lattice relaxation rates for 2,5tASQ in 1:4 glycerol:ethanol, 1:1 glycerol:ethanol, and triethanolamine between 25 and 295 K (Fig. 2) are typical of the semiquinones studied. Although relaxation rates change monotonically with temperature,

Table 2
Parameters used to model the temperature dependence of relaxation rates at X-band[a].

Radical	Solvent	g value ±0.0001	C_{dir} (s^{-1})	C_{Ram}[b] ($\times10^3 s^{-1}$)	C_{loc}[c] ($\times10^6 s^{-1}$)	$C_{g,A}$ ($\times10^{15}$ s^{-2})	α
2,5PSQ	1:4 glycerol: ethanol	g_x = 2.0067 g_y = 2.0051 g_z = 2.0023	0.3	12.6	0.127	1.69	1.5
2,5tASQ	1:4 glycerol: ethanol	g_x = 2.0064 g_y = 2.0053 g_z = 2.0023	0.4	14.9	0.17	1.567	1.45
2,5tBSQ	1:4 glycerol: ethanol	g_x = 2.0065 g_y = 2.0052 g_z = 2.0023	0.3	15.5	0.175	1.571	1.23
2,6tBSQ	1:4 glycerol: ethanol	g_x = 2.0064 g_y = 2.0052 g_z = 2.0023	0.65	16.9	0.18	1.493	1.23
2,5tASQ	1:1 glycerol: ethanol	g_x = 2.0064 g_y = 2.0053 g_z = 2.0023	0.45	13.3	0.127	1.567	1.45
2,5tBSQ	1:1 glycerol: ethanol	g_x = 2.0065 g_y = 2.0052 g_z = 2.0023	0.45	13.7	0.131	1.571	1.23
2,6tBSQ	1:1 glycerol: ethanol	g_x = 2.0064 g_y = 2.0052 g_z = 2.0023	0.7	15.4	0.142	1.492	1.23
2,5PSQ	Triethanolamine		0.4	10.8	0.089		
2,5tASQ	Triethanolamine		0.41	12.4	0.107		
2,5tBSQ	Triethanolamine		0.41	12.8	0.110		
2,6tBSQ	Triethanolamine		0.56	14.7	0.128		
THSQ	Triethanolamine		0.1	15	0.129		

[a] Relaxation rates were measured at the position of maximum intensity of the absorption signal.
[b] Debye temperature fixed at 150 K.
[c] Energy of local mode fixed at 600 K.

the temperature dependence could not be modeled with a single relaxation process. Between about 35 and 80 K the Raman process dominates. Below about 35 K the temperature dependence of $1/T_1$ could not be fitted with the Raman process alone, which required inclusion of a contribution with the linear temperature dependence that is characteristic of the direct process (Eq. (1)). Above about 80 K $\log(1/T_1)$ vs. $\log T$ would have a slope of 2, if it followed the high temperature limiting form of the Raman process (Eq. (3)). However, the slope is greater than 2, which indicates that an additional process contributes. The basis for assignment of that process as a local mode is discussed below. In highly viscous triethanolamine, contributions from the direct, Raman, and local-mode processes are sufficient to model the temperature dependence of $1/T_1$ over the full temperature range studied (Fig. 2). In the least viscous solvent, 1:4 glycerol:ethanol, relaxation rates above 230 K were faster than in the more viscous solvents, which is attributed to tumbling-dependent processes.

3.2. Orientation dependence of $1/T_1$

The X-band CW EPR spectrum of 2,6tBSQ in 1:4 glycerol:ethanol at 85 K is a single broad line with peak to peak line width of 5.5 G (Fig. 3a). Although g anisotropy is not resolved at X-band, at Q-band resonance for g_{zz} (2.0023) is well resolved from g_{xx} (2.0064) and g_{yy} (2.0052) (Fig. 3b). The g values for the other semiquinones are similar to those of 2,6tBSQ (Table 2). Because of the g value resolution, the dependence of spin lattice relaxation rates at 85 K on position in the spectrum is better resolved at Q-band than at X-band (Fig. 3a and b). The relaxation rates are 2.7–1.5 times faster near the g_{xx} ($g \sim 2.006$) and g_{yy} ($g \sim 2.005$) axes than along the g_{zz} axis ($g \sim 2.0023$). Slower relaxation along the g_{zz} axis, which has the smallest g value, also has been observed for nitroxyl radicals [53]. Anisotropy of vibrational modes or of spin–orbit coupling may contribute to orientation dependence of relaxation [53].

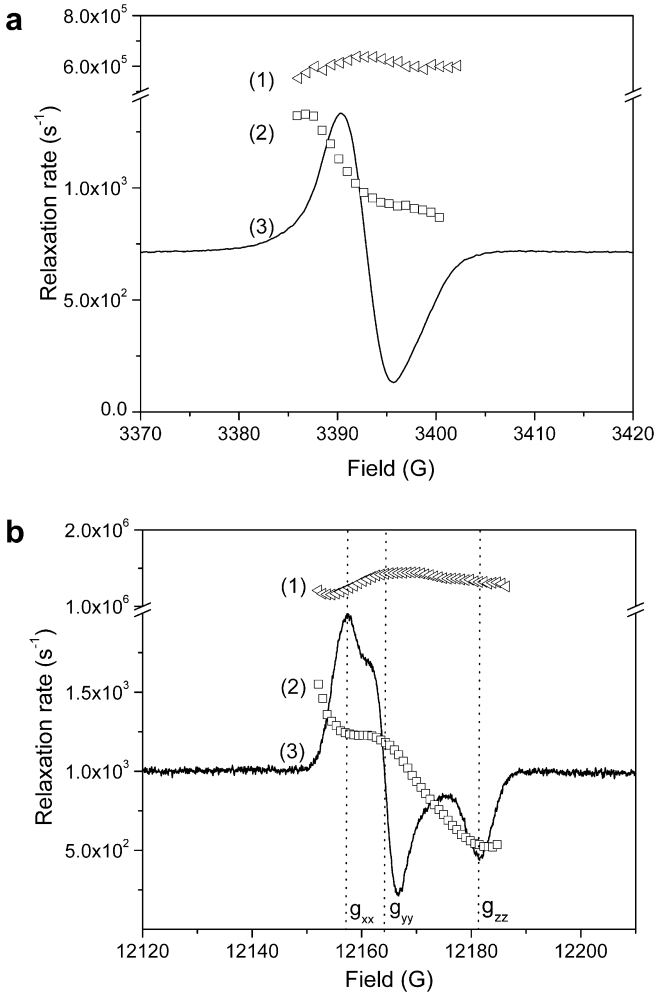

Fig. 3. (a) X-band data for 2,6tBSQ in 1:4 glycerol: ethanol at 85 K. (1) Orientation dependence of $1/T_m$, (2) orientation dependence of $1/T_1$ obtained by inversion recovery, and (3) CW EPR spectrum. (b) Q-band data for 2,6tBSQ in 1:4 glycerol: ethanol at 85 K. (1) Orientation dependence of $1/T_m$, (2) orientation dependence of $1/T_1$ obtained by inversion recovery, and (3) CW EPR spectrum.

3.3. Frequency dependence of $1/T_1$

The temperature dependence between 85 and 295 K of $1/T_1$ in triethanolamine at X and Q-band for 2,5tASQ and THSQ is shown in Fig. 4a and b, respectively. Rates at S-band at 293 K are also

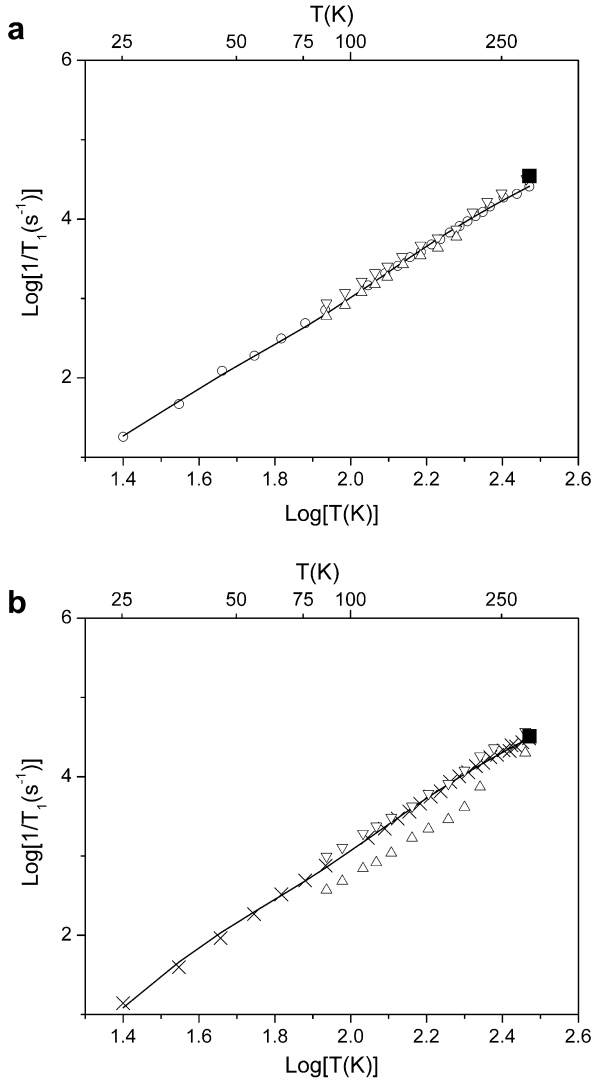

Fig. 4. (a) Temperature dependence of spin lattice relaxation rates for 2,5tASQ in triethanolamine at X-band (○), at Q-band along the g_{yy} axis (▽), at Q-band along the g_{zz} axis (△), and at S-band (■). (b) Temperature dependence of spin lattice relaxation rates for THSQ in triethanolamine at X-band (×), at Q-band along the g_{yy} axis (▽), at Q-band along the g_{zz} axis (△), and at S-band (■). The solid lines are the fit functions for the X-band data. It is assumed that the temperature dependence that is characteristic of the Raman and local modes in glasses persists above the glass transition temperature.

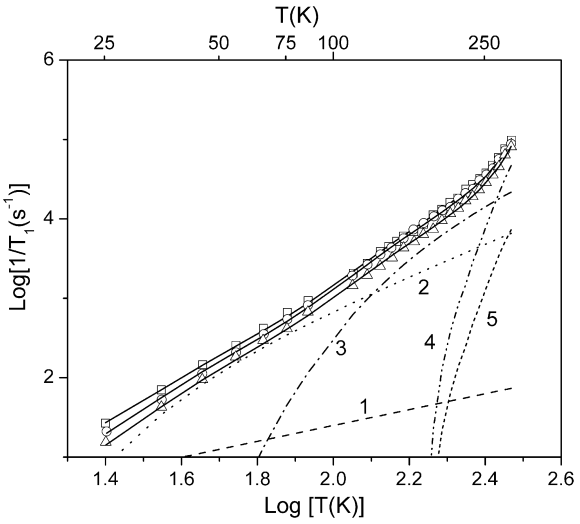

Fig. 5. Temperature dependence of relaxation rates for 2,6tBSQ (□), 2,5tASQ (○), and 2,5PSQ (△) in 1:4 glycerol:ethanol. The solid line is the fit function which is the sum of contributions that are shown as dashed lines for the direct (1), Raman (2), local mode (3), spin rotation (4), and modulation of g and A processes (5). It is assumed that the temperature dependence that is characteristic of the Raman and local modes in glasses persists above the glass transition temperature.

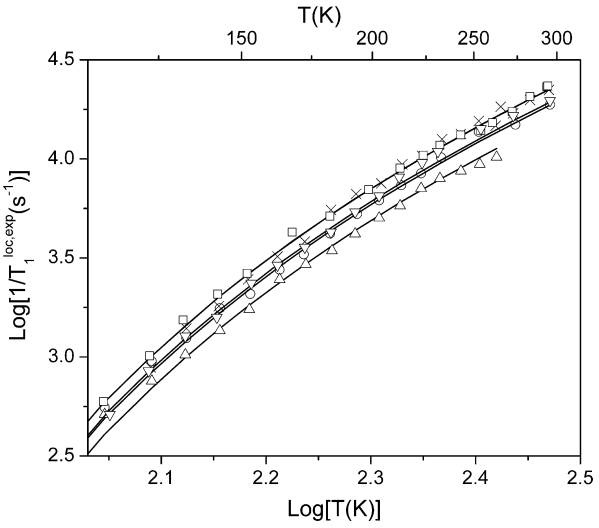

Fig. 6. Contributions to spin–lattice relaxation rates from the local mode as a function of temperature for semiquinones in triethanolamine: 2,5tBSQ (▽), 2,5tASQ (○), 2,5PSQ (△), 2,6tBSQ (□), THSQ (×). The solid lines are the fit functions.

shown. At Q-band, throughout the temperature range studied, rates for 2,5tASQ are about 20% faster along g_{yy} and about 20% slower along g_{zz} than in the center of the spectrum at X-band. For THSQ the rates measured at X-band along the $g_{\perp}$ axis are similar to the rates measured at Q-band along g_{yy}, which are about twice as fast as along g_{zz} at Q-band (Fig. 4b). At room temperature rates at S-band are within experimental uncertainty of rates at X-band. Since the differences between rates at X-band and Q-band are small and temperature independent, they are attributed to better resolution of the orientation dependence of $1/T_1$ at Q-band than at X-band, and not to frequency dependence of the process. Hence, the process is assigned as a local mode.

3.4. Impact of semiquinone structure on contributions to $1/T_1$

Relaxation rates in 1:4 glycerol:ethanol between 25 and 295 K show systematic differences between semiquinones (Fig. 5), although the overall dependence on temperature is similar. These differences are reflected in the coefficients for the contributions from the relaxation processes that are summarized in Table 2.

3.4.1. Direct process

The values of C_{dir} are between 0.1 and 0.7, are not strongly solvent dependent, and increase in the order THSQ <2,5-substituted semiquinones <2,6tBSQ. Ion pairing of semiquinones with alkali metals [54–56] may contribute to locally high concentrations that enhance the direct process [13]. The large variations in C_{dir} may be due to differences in stacking, with the most negatively charged THSQ having the smallest tendency to stack. Differences in spin density distributions may also contribute to variations in C_{dir}.

3.4.2. Raman process

The trends in C_{Ram} are the same for the three solvents: 2,5PSQ (mw = 260) < 2,5tASQ (mw = 250) < 2,5tBSQ (mw = 220) < 2,6tBSQ (mw = 220) < THSQ (mw = 172). The relaxation rates increase approximately inversely proportional to molar mass, which is similar to what has been observed for nitroxyl radicals [12]. Although the molar masses are the same, the relaxation rates are faster for 2,6tBSQ than for 2,5tBSQ. The proton hyperfine couplings in 2,5tBSQ to the ring protons (2.15 G) and to the t-butyl protons (0.056 G) are larger than the corresponding couplings for 2,6tBSQ: 1.24 G and 0.052 G. These differences in coupling constants indicate that in the 2,5-substituted semiquinone, the spin density is enhanced at the 2,3,5,6 positions of the ring at the expense of the 1,4 positions and oxygens. Since the Raman process is a vibration-related process, changes in the spin density distributions that modify the impact of individual vibrations on the unpaired electron, impact spin lattice relaxation. The lower spin density on the 1,4 positions decreases spin–orbit coupling for 2,5tBSQ, which decreases the spin–lattice relaxation rate.

3.4.3. Local mode

In triethanolamine, tumbling is so slow that even at room temperature the tumbling-dependent processes make negligible contributions to the spin lattice relaxation (Fig. 2), so relaxation rates in this solvent were chosen to examine the local mode in greater detail. The contributions from the local mode, $\frac{1}{T_1^{loc,exp}}$, were estimated from the experimental rates by subtracting the contributions from the direct, $\frac{1}{T_1^{dir}}$, and Raman, $\frac{1}{T_1^{Ram}}$, processes calculated

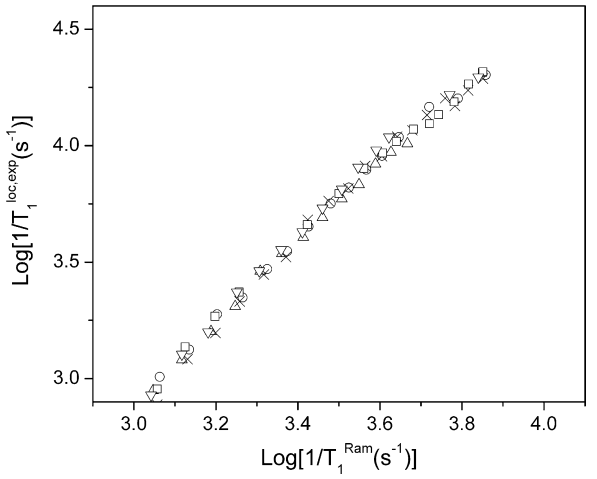

Fig. 7. Correlation between the experimental contributions from the Raman and local-mode processes in triethanolamine for 2,5tBSQ (▽), 2,5tASQ (○), 2,5PSQ (△), 2,6tBSQ (□), and THSQ (×). To obtain this master curve the values added to the x and y coordinates were 0.07 for 2,5PSQ, 0.03 for 2,5tASQ, −0.05 for 2,6tBSQ, and −0.06 for THSQ.

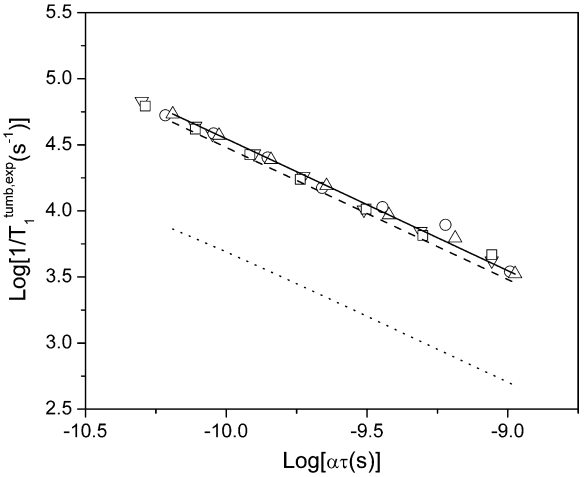

Fig. 8. Dependence, between 295 and 233 K, of contributions to spin–lattice relaxation from the tumbling-dependent processes on tumbling correlation time in 1:4 glycerol:ethanol for 2,5tBSQ (▽), 2,5tASQ (○), 2,5PSQ (△), 2,6tBSQ (□). The solid line is the sum of contributions from spin rotation (--) and modulation of *g* and *A* anisotropy (. . .) for 2,5PSQ.

using the parameters in Table 2 at each temperature (Eq. (14)). The resulting values are shown in Fig. 6.

$$\frac{1}{T_1^{\mathrm{loc,exp}}} = \frac{1}{T_1} - \frac{1}{T_1^{\mathrm{dir}}} - \frac{1}{T_1^{\mathrm{Ram}}} \tag{14}$$

The temperature dependence of $\frac{1}{T_1^{\mathrm{loc,exp}}}$ is similar for the five semiquinones and C_{loc} increases in the order 2,5PSQ < 2,5tASQ ~ 2,5tBSQ <2,6tBSQ ~ THSQ (Table 2), which is similar to the trends observed for C_{Ram}. The contributions to relaxation from the local mode are plotted against the contributions from the Raman process in Fig. 7. For each semiquinone a constant value was added to both the *x* and *y* coordinates to scale the values to overlay the curve for 2,5tBSQ. On this master curve the contributions from the two processes are proportional throughout the accessible temperature region, which means that if θ_{D} and Δ_{local} are constant, C_{Ram} is proportional to C_{local}. This observation indicates that similar factors impact both two-phonon processes. Similar correlations were observed in other solvents. A correlation between the contributions from the Raman and local-mode processes also was observed for nitroxyl radicals [12].

In highly viscous triethanolamine, tumbling-dependent processes make negligible contribution to relaxation and there is no change in the slope of the plot of $\log(1/T_1)$ vs. $\log T$ (Figs. 2 and 4a and b) in the vicinity of the glass transition temperature. This implies that processes with the temperature dependence that is characteristic of the Raman and local mode in the glassy state contribute to relaxation in fluid solution.

3.4.4. Tumbling-dependent processes

The contributions to the experimental rates from the tumbling-dependent processes were determined by subtracting the contributions from the direct, Raman, and local-mode processes calculated using the parameters in Table 2 at each temperature

$$\frac{1}{T_1^{\mathrm{tumb,exp}}} = \frac{1}{T_1} - \frac{1}{T_1^{\mathrm{dir}}} - \frac{1}{T_1^{\mathrm{Ram}}} - \frac{1}{T_1^{\mathrm{loc}}} \tag{15}$$

Values of $\frac{1}{T_1^{\mathrm{tumb,exp}}}$ for the four semiquinones that could be studied in 1:4 glycerol:ethanol are proportional to $\alpha\tau$, which corrects for differences in molar masses (Fig. 8). As indicated by the fit lines, the contribution from spin rotation is much larger than from modulation of *g* and *A* anisotropy [42–44,46,47].

3.4.5. Negligible impact of methyl groups

The relaxation rates for all of the methyl-containing semiquinones were slower than for THSQ, which contains no methyl groups. Thus there is no indication of T_1 relaxation enhancement by rotation of methyl groups.

3.5. Comparison with relaxation processes for nitroxyl radicals

Throughout the temperature range studied relaxation rates for the semiquinones are slower than for nitroxyl radicals [8,12,14]. The isotropic *g* values for semiquinones are 2.0046–2.0051 which are substantially smaller then the $g \sim 2.006$ for nitroxyls, so the slower relaxation rates for the semiquinones are attributed to smaller spin–orbit coupling [12], which influences all of the relaxation process, except the direct process. The proton hyperfine couplings of the semiquinones (Table 2) are much smaller than the nitrogen hyperfine couplings of the nitroxyl (A_{xx} = 5.9 G, A_{yy} = 4.3 G, A_{zz} = 33.2 G for tempone in 1:4 glycerol:ethanol). The coefficient $C_{A,g}$ *(Eq. (8))* is about $1.5 \times 10^{15}\ \mathrm{s}^{-2}$ for semiquinones (Table 2), which is more than an order of magnitude smaller that the value of about $9 \times 10^{16}\ \mathrm{s}^{-2}$ for nitroxyls [14]. The contribution to relaxation from spin rotation (Eqs. (6) and (12)) is proportional to the coefficient $\sum_{i=1}^{3} \frac{(g_i - g_e)^2}{9}$. This factor is about 3×10^{-6} for semiquinones, which is only about a factor of two smaller than the value of about 7×10^{-6} for nitroxyls. Although modulation of *A* anisotropy dominates the tumbling-dependent contribution to relaxation for nitroxyl radicals at X-band, the much smaller decrease in the coefficient for the spin rotation process than in the coefficient $C_{A,g}$ means that the spin-rotation contribution is the dominant tumbling-dependent contribution for semiquinones, as concluded in prior studies [42–44,46,47]. The modulation of *g* and *A* anisotropy makes negligible contribution to the relaxation for the semiquinones.

3.6. Spin echo dephasing rates ($1/T_m$)

Spin echo dephasing experiments can elucidate the dynamics of the methyl groups and provide information that is not available from spin lattice relaxation. The spin echo dephasing rate ($1/T_{\mathrm{m}}$) includes the effects of all process that take spins off resonance: instantaneous diffusion, fluctuation of dipolar interactions, libra-

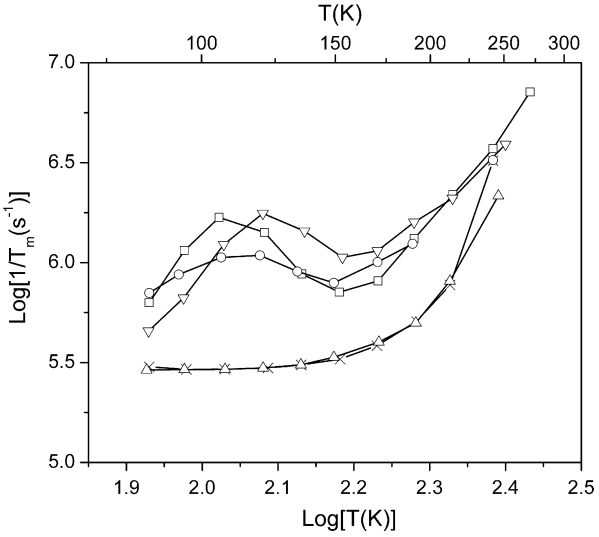

Fig. 9. Temperature dependence of spin echo dephasing rates in triethanolamine for 2,5PSQ (△), THSQ (×), 2,5tASQ (○), 2,6tBSQ (□), and 2,5tBSQ (▽).

tional motion of the paramagnetic species and nuclear spin diffusion [8].

3.6.1. Temperature dependence of $1/T_m$

The echo decay curves for 2,5tASQ, 2,5tBSQ, and 2,6tBSQ in triethanolamine could be fit well with the function $Y(\tau) = Y(0)\exp[(\frac{2\tau}{T_m})^n] + C$ with $n = 1$, which is observed when a dynamic process occurs on the time scale of the experiment [57]. Echo decay curves for 2,5PSQ and THSQ below 150 K could be fit better with $n = 2$, which is observed when nuclear spin diffusion dominates [57]. To facilitate comparisons, $n = 1$ was used to obtain the values of $1/T_m$ that are shown in Figs. 3a and b and 9 for all samples. The temperature dependence of $1/T_m$ is substantially different for 2,5PSQ and THSQ, which do not contain methyl groups, than for the semiquinones that have methyl groups (Fig. 9). In nitroxyl radicals and Cr(V) complexes rotation of ring methyl groups at rates comparable to inequivalences in the electron–proton couplings enhances spin echo dephasing at temperatures between about 80 and 175 K [8,58,59]. By analogy, the enhanced dephasing rates between about 80 and 160 K for the t-butyl or t-amyl containing semiquinones is attributed to rotation of methyl groups. As the temperature is increased above 150 K, the dephasing rates became faster for all of the radicals, which is attributed to increased molecular motion as the glass softens. The maximum enhancement of $1/T_m$ occurs at higher temperatures for molecules with higher activation energies [59], which indicates that the activation energies are in the order 2,5tBSQ > 25tASQ > 26tBSQ. The higher activation energy for 2,5tBSQ than for 2,5tASQ is consistent with increased steric hindrance in a t-butyl group than in a t-amyl group. The higher activation energy for 2,5tBSQ than for 2,6tBSQ (Fig. 9) can be explained by considering the activation energies for rotation of the methyl groups of 1-hydroxy-2,4,6 tri-t-butylbenzene and 1-hydroxy-2,5-di-t-butylbenzene. The activation energy for reorientation of two c type methyl group and one b type methyl group of the B type t-butyl groups of 1-hydroxy-2,4,6 tri-t-butylbenzene and 1-hydroxy-2,5-di-t-butylbenzene are 10, 20 kJ $mol^{-1}$and 15, 28 kJ mol^{-1} [60]. With respect to the molecular symmetry, the B type t-butyl groups at the 2 and 6 position of 1-hydroxy-2,4,6 tri-t-butylbenzene are equivalent to the B type t-butyl groups at the 2 and 6 position of 2,6tBSQ. The B type t-butyl groups at position 2 of 1-hydroxy-2,5-di-t-butylbenzene are equivalent to the B type t-butyl groups at the 2 and 5 position of 2,5tBSQ. Based on this analogy the activation energy for reorientation of the methyl groups of 2,6tBSQ are expected to be much smaller than for 2,5tBSQ.

3.6.2. Orientation dependence of $1/T_m$

The spin echo dephasing rate also depends on position in the EPR spectrum, which can be seen more clearly at Q-band than at X-band (Fig. 3a and b). The spin echo dephasing rate is faster near the center of the spectrum than at either extreme. This field dependence is characteristic of the impact of molecular motion on $1/T_m$ [61], which is smaller along the principal axes and larger for intermediate orientations. Movement of the spin off resonance is a dephasing process. In the CW spectrum g_{yy} is not well resolved from g_{xx} and hence the field dependence is not clear around the g_{yy} axis, but has greater impact at positions intermediate between g_{zz} and g_{yy}.

4. Conclusions

The electron spin–lattice relaxation rates of semiquinones between 25 and 295 K in highly viscous triethanolamine can be modeled with contributions from the direct, Raman, and local-mode processes. The contributions from the Raman and local-mode processes are correlated (Fig. 7). The higher spin density on the 1,4 positions and oxygens for 2,6tBSQ than for 2,5-disubstituted semiquinones results in faster relaxation by the Raman, and local-mode processes. Near room temperature in lower viscosity 1:4 glycerol:ethanol and 1:1 glycerol:ethanol spin rotation makes significant contributions to the relaxation. Spin lattice relaxation rates for semiquinones are slower than for nitroxyl radicals at all temperatures studied, which is attributed to smaller spin–orbit coupling. Because of the much smaller hyperfine couplings, the dominant tumbling-dependent relaxation process for semiquinones is spin rotation, instead of the modulation of g and A anisotropy that dominates for nitroxyls.

Acknowledgment

Support from NIH NIBIB Grant EB002807 is gratefully acknowledged.

References

[1] S.S. Eaton, G.R. Eaton, Determination of distances based on T_1 and T_m effects, Biol. Magn. Reson. 19 (2000) 347–381.
[2] M. Plato, W. Lubitz, K. Mobius, A solution ENDOR sensitivity study of various nuclei in organic radicals, J. Phys. Chem. 85 (1981) 1202–1219.
[3] M. Persson, J.R. Harbridge, P. Hammarstrom, R. Mitri, L.-G. Martensson, U. Carlsson, G.R. Eaton, S.S. Eaton, Comparison of electron paramagnetic resonance methods to determine distances between spin labels on human carbonic anhydrase II, Biophys. J. 80 (2001) 2886–2897.
[4] A. Abragam, B. Bleaney, Electron Paramagnetic Resonance of Transition Ions, Oxford University Press, Oxford, 1970.
[5] C.P. Poole, H. Farach, Relaxation in Magnetic Resonance, Academic Press, New York, 1971.
[6] K.J. Standley, R.A. Vaughan, Electron Spin Relaxation Phenomena in Solids, Plenum Press, 1969.
[7] Y. Zhou, B.E. Bowler, G.R. Eaton, S.S. Eaton, Electron spin lattice relaxation rates for $S = 1/2$ molecular species in glassy matrices or magnetically dilute solids at temperatures between 10 and 300 K, J. Magn. Reson. 139 (1999) 165–174.
[8] S.S. Eaton, G.R. Eaton, Relaxation times of organic radicals and transition metal ions, Biol. Magn. Reson. 19 (2000) 29–154.
[9] M.K. Bowman, L. Kevan, Electron spin–lattice relaxation in non-ionic solids, in: L. Kevan, R.N. Schwartz (Eds.), Time Domain Electron Spin Resonance, John Wiley, New York, 1979, pp. 68–105.
[10] L. Yong, J. Harbridge, R.W. Quine, G.A. Rinard, S.S. Eaton, G.R. Eaton, C. Mailer, E. Barth, H.J. Halpern, Electron spin relaxation of triarylmethyl radicals in fluid solution, J. Magn. Reson. 152 (2001) 156–161.
[11] A.J. Fielding, P.J. Carl, G.R. Eaton, S.S. Eaton, Multifrequency EPR of four triarylmethyl radicals, Appl. Magn. Reson. 28 (2005) 239–249.
[12] H. Sato, V. Kathirvelu, A.J. Fielding, S.E. Bottle, J.P. Blinco, A.S. Micallef, S.S. Eaton, G.R. Eaton, Impact of molecular size on electron spin relaxation rates of nitroxyl radicals in glassy solvents between 100 and 300 K, Mol. Phys. 105 (2007) 2137–2151.
[13] H. Sato, V. Kathirvelu, G. Spagnol, S. Rajca, S.S. Eaton, G.R. Eaton, Impact of electron–electron spin interaction on electron spin relaxation of nitroxide diradicals and tetraradical in glassy solvents between 10 and 300 K, J. Phys. Chem. B. 112 (2008) 2818–2828.
[14] H. Sato, S.E. Bottle, J.P. Blinco, A.S. Micallef, G.R. Eaton, S.S. Eaton, Electron spin–lattice relaxation of nitroxyl radicals in temperature ranges that span glassy solutions to low-viscosity liquids, J. Magn. Reson. 191 (2008) 66–77.
[15] A.J. Fielding, S. Fox, G.L. Millhauser, M. Chattopadhyay, P.M.H. Kroneck, G. Fritz, G.R. Eaton, S.S. Eaton, Electron spin relaxation of copper(II) complexes in glassy solution between 10 and 120 K, J. Magn. Reson. 179 (2006) 92–104.
[16] A.J. Fielding, D.B. Back, M. Engler, B. Baruah, D.C. Crans, G.R. Eaton, S.S. Eaton, Electron spin lattice relaxation of V(IV) complexes in glassy solutions between 15 and 70 K, ACS Symp. Series 974 (2007) 364–375.
[17] S.S. Eaton, J. Harbridge, G.A. Rinard, G.R. Eaton, R.T. Weber, Frequency dependence of electron spin relaxation for three $S = 1/2$ species doped into diamagnetic solid hosts, Appl. Magn. Reson. 20 (2001) 151–157.
[18] J.W. Orton, Electron Paramagnetic Resonance: an Introduction to Transition Group Ions in Crystals, Gordon and Breach, 1968.
[19] J. Murphy, Spin–lattice relaxation due to local vibrations with temperature-independent amplitudes, Phys. Rev. 145 (1966) 241–247.
[20] J.H. Van Vleck, Paramagnetic relaxation and the equilibrium of lattice oscillators, Phys. Rev. 59 (1941) 724–729.
[21] M. Kveder, D. Merunka, A. Ilakovac, J. Makarevic, M. Jokic, B. Rakvin, Direct evidence for the glass-crystalline transformation in solid ethanol by means of a nitroxide spin probe, Chem. Phys. Lett. 419 (2006) 91–95.
[22] J.G. Castle Jr., D.W. Feldman, Temperature dependence of paramagnetic relaxation at point defects in vitreous silica, J. Appl. Phys. 36 (1965) 124–128.
[23] J.R. Harbridge, S.S. Eaton, G.R. Eaton, Electron spin–lattice relaxation in radicals containing two methyl groups, generated by γ-irradiation of polycrystalline solids, J. Magn. Reson. 159 (2002) 195–206.

[24] J.R. Harbridge, S.S. Eaton, G.R. Eaton, Electron spin–lattice relaxation processes of radicals in irradiated crystalline organic compounds, J. Phys. Chem. A 107 (2003) 598–610.
[25] S. Clough, F. Poldy, Study of tunneling rotation of methyl groups by electron spin resonance and electron nuclear double resonance, J. Chem. Phys. 51 (1969) 2076–2087.
[26] S. Clough, J.R. Hill, Tunnelling resonance in electron spin–lattice relaxation, J. Phys. C Solid State Phys. 8 (1975) 2274–2282.
[27] P.W. Atkins, Spin–rotation interaction, in: L.T. Muus, P.W. Atkins (Eds.), Electron Spin Relaxation in Liquids, Plenum Press, New York, 1972, pp. 279–312.
[28] B.H. Robinson, D.A. Haas, C. Mailer, Molecular dynamics in liquids: spin–lattice relaxation of nitroxide spin labels, Science 263 (1994) 490–493.
[29] B.H. Robinson, A.W. Reese, E. Gibbons, C. Mailer, A unified description of the spin–spin and spin–lattice relaxation rates applied to nitroxide spin labels in viscous liquids, J. Phys. Chem. B 103 (1999) 5881–5894.
[30] R. Owenius, G.E. Terry, M.J. Williams, S.S. Eaton, G.R. Eaton, Frequency dependence of electron spin relaxation of nitroxyl radicals in fluid solution, J. Phys. Chem. B 108 (2004) 9475–9481.
[31] C. Mailer, R.D. Nielsen, B.H. Robinson, Explanation of spin–lattice relaxation rates of spin labels obtained with multifrequency saturation recovery EPR, J. Phys. Chem. A 109 (2005) 4049–4061.
[32] L. Andreozzi, M. Faetti, M. Giordano, D. Leporini, Scaling of the rotational relaxation of tracers in *o*-terphenyl: a linear and nonlinear ESR study, J. Phys. Chem. B. 103 (1999) 4097–4103.
[33] B.H. Robinson, C. Mailer, A.W. Reese, Linewidth analysis of spin labels in liquids. I. Theory and data analysis, J. Magn. Reson. 138 (1999) 199–209.
[34] B.H. Robinson, C. Mailer, A.W. Reese, Linewidth analysis of spin labels in liquids. II. Experimental, J. Magn. Reson. 138 (1999) 210–219.
[35] D.E. Budil, S. Lee, S. Saxena, J.H. Freed, Nonlinear least-squares analysis of slow-motion EPR spectra in one and two dimensions using a modified Levenberg–Marquardt algorithm, J. Magn. Reson. A 120 (1996) 155–189.
[36] C. Mailer, B.H. Robiinson, D.A. Haas, New developments in pulsed electron paramagnetic resonance: relaxation mechanisms of nitroxide spin labels, Bull. Magn. Reson. 14 (1992) 30–35.
[37] R. Owenius, G.R. Eaton, S.S. Eaton, Frequency (250 MHz to 9.2 GHz) and viscosity dependence of electron spin relaxation of triarylmethyl radicals at room temperature, J. Magn. Res. 172 (2005) 168–175.
[38] S. Deller, P. Macheroux, S. Sollner, Flavin-dependent quinone reductases, Cell. Mol. Life Sci. 65 (2008) 141–160.
[39] S.E.J. Rigby, J. Basran, J.P. Combe, A.W. Mohsen, H.S. Toogood, A. van Thiel, M.J. Sutcliffe, D. Leys, A.W. Munro, N.S. Scrutton, Flavoenzyme catalysed oxidation of amines: role of flavin and protein-based radicals, Biochem. Soc. Trans. 33 (2005) 754–757.
[40] A.J. Fielding, R.J. Usselman, N. Watmough, M. Simkovic, F.E. Frerman, G.R. Eaton, S.S. Eaton, Electron paramagnetic resonance characterization and interspin distance measurement of electron transfer flavoprotein ubiquinone oxidoreductase (ETF-QO), J. Magn. Reson. 190 (2008) 222–232.
[41] R.J. Usselman, A.J. Fielding, F.E. Frerman, G.R. Eaton, S.S. Eaton, Impact of mutations on the midpoint potential of the $[4Fe\text{-}4S]^{+}$ cluster and on the catalytic activity in electron transfer flavoprotein-ubiquinone oxidoreductase (ETF-Qo), Biochemistry 47 (2008) 92–100.
[42] S.K. Rengan, M.P. Khakhar, B.S. Prabhananda, B. Venkataraman, Electron spin–lattice relaxation in organic free radicals in solutions, Pure Appl. Chem. 32 (1972) 287–305.
[43] S.K. Rengan, M.P. Khakhar, B.S. Prabhananda, B. Venkataraman, Study of molecular motions in liquids by electron spin–lattice relaxation measurements. I. Semiquinone ions in hydrogen bonding solvents, Pramana 3 (1974) 95–121.
[44] S.K. Rengan, M.P. Khakhar, B.S. Prabhananda, B. Venkataraman, Study of molecular motions in liquids by electron spin–lattice relaxation measurements. II. 2,5-Di-tert-butylsemiquinone ions in acetonitrile and tetrahydrofuran, J. Magn. Reson. 16 (1974) 35–43.
[45] K.V. Lingam, P.G. Nair, B. Venkataraman, Spin–lattice relaxation studies of semiquinone ions, Proc. Indian Acad. Sci. A 76 (1972) 207–220.
[46] B.S. Prabhananda, J.S. Hyde, Study of molecular motions in liquids by electron spin relaxation: halogenated *p*-semiquinone anions in alcohols, J. Chem. Phys. 85 (1986) 6705–6712.
[47] G. Krishnamoorthy, B.S. Prabhananda, Molecular motions in liquidlike pockets of frozen solutions: electron spin relaxation study of semiquinones in DMSO and DMSO-ethanol mixtures, J. Chem. Phys. 76 (1982) 108–113.
[48] D.S. Leniart, H.D. Connor, J.H. Freed, An ESR and ENDOR study of spin relaxation of semiquinone in liquid solution, J. Chem. Phys. 63 (1975) 165–199.
[49] V. Kathirvelu, H. Sato, R.W. Quine, G.A. Rinard, S.S. Eaton, G.R. Eaton, EPR free induction decay coherence observed after a single-pulse in saturation recovery experiments for samples with resolved multi-line CW spectra, Appl. Magn. Reson. 32 (2007) 269–281.
[50] R.W. Quine, G.R. Eaton, S.S. Eaton, Pulsed EPR spectrometer, Rev. Sci. Instrum. 58 (1987) 1709–1723.
[51] R.W. Quine, G.A. Rinard, B.T. Ghim, S.S. Eaton, G.R. Eaton, A 1–2 GHz pulsed and continuous wave electron paramagnetic resonance spectrometer, Rev. Sci. Instrum. 67 (1996) 2514–2527.
[52] N. Davidson, R.H. Cole, Dielectric relaxation in glycerol, propylene glycol, and *n*-propanol, J. Chem. Phys. 19 (1951) 1484–1490.
[53] J.-L. Du, G.R. Eaton, S.S. Eaton, Temperature, orientation, and solvent dependence of electron spin–lattice relaxation rates for nitroxyl radicals in glassy solvents and doped solids, J. Magn. Reson. A 115 (1995) 213–221.
[54] J.-M. Lue, S.V. Rosokha, I.S. Neretin, J.K. Kochi, Quinones as electron acceptors. X-ray structures, spectral (EPR, UV–vis) characteristics and electron-transfer reactivities of their reduced anion radicals as separated vs. contact ion pairs, J. Am. Chem. Soc. 128 (2006) 16708–16719.
[55] L. Pasimeni, M. Brustolon, C. Corvaja, Electron spin resonance investigation of *o*-chloranil alkali metal ion pairs, J. Magn. Reson. 21 (1976) 259–269.
[56] T. Fujinaga, S. Okazaki, T. Nagaoka, Ion pair formation between electro-generated 1,2-naphthoquinone anion radicals and alkali metal cations in acetonitrile, Bull. Chem. Soc. Jpn. 53 (1980) 2241–2247.
[57] I.M. Brown, Electron spin echo studies of relaxation processes in molecular solids, in: L. Kevan, R.N. Schwartz (Eds.), Time Domain Electron Spin Resonance, John Wiley, New York, 1979, pp. 195–229.
[58] S.A. Dzuba, A.G. Maryasov, A.K. Salikhov, Y.D. Tsvetkov, Super slow rotations of nitroxide radicals studied by pulse EPR spectroscopy, J. Magn. Reson. 58 (1984) 95–117.
[59] K. Nakagawa, M.B. Candelaria, W.W.C. Chik, S.S. Eaton, G.R. Eaton, Electron-spin relaxation times of chromium(V), J. Magn. Reson. 98 (1992) 81–91.
[60] P.A. Beckmann, H.A. Al-Hallaq, A.M. Fry, A.L. Plofker, B.A. Roe, J.A. Weiss, Solid state proton spin relaxation and methyl and *t*-butyl reorientation, J. Chem. Phys. 100 (1994) 752.
[61] J.L. Du, K.M. More, S.S. Eaton, G.R. Eaton, Orientation dependence of electron spin phase memory relaxation times in copper(II) and vanadyl complexes in frozen solution, Israel J. Chem. 32 (1992) 351–355.